

Helicity, assembly, and circularly polarized luminescence of chiral AIEgens

Hongkun Li,^{a,b,c} Bing Shi Li,^{b,*} Ben Zhong Tang^{a,*}

^aThe Hong Kong University of Science & Technology, Department of Chemistry, Jockey Club Institute for Advanced Study, Institute of Molecular Functional Materials, State Key Laboratory of Molecular Neuroscience, Division of Biomedical Engineering, and Hong Kong Branch of Chinese National Engineering Research Center for Tissue Restoration and Reconstruction (CNERC-HK Branch), Clear Water Bay, Kowloon, Hong Kong, China. E-mail: tangbenz@ust.hk

^bShenzhen University, College of Chemistry and Environmental Engineering, Key Laboratory of New Lithium-Ion Battery and Mesoporous Material, Shenzhen 518060, China. E-mail: phbingsl@szu.edu.cn

^cSoochow University, College of Chemistry, Chemical Engineering and Materials Science, Laboratory of Advanced Optoelectronic Materials, Suzhou 215123, China

ABSTRACT. As opposed to most fluorophores that suffer from aggregation-caused quenching (ACQ), aggregation-induced emissive luminogens (AIEgens) possess very weak fluorescence in solution, but show strong emission upon aggregation due to restriction of intramolecular motion (RIM). Since AIEgens are often comprised of propeller-shaped structures, i.e. polyphenylsiloles or tetraphenylethylene (TPE), the attachment of chiral units has recently proven a powerful tool to fabricate chiral AIEgens exhibiting strong circularly-polarized luminescence (CPL) signal upon aggregation. Different chiral moieties lead to various assembled structures, such as helical nanoribbons, superhelical ropes, hollow and solid micro-/nanospheres. Generally, these structures exhibit enhanced chiroptical properties when compared to their monomeric counterpart. In this context, we report on the tetraphenylsilole and TPE derivatives with side-chains bearing an enantiomerically pure chiral units readily assembled into superhelical ropes upon aggregation, which displayed large CPL dissymmetry factors (g_{em}) of -0.32 – a record for purely organic chiral materials.

1 INTRODUCTION

Chirality is universal in nature and expressed at hierarchical levels. The chirality at molecular and supramolecular level is of pivotal importance because it is closely related with the chemical, physical and biological functions of the molecules, as best exemplified with chiral amino acids. Hybridization of chirality with π -conjugated molecules usually leads to chiroptical properties, which have important application as optoelectronics devices and chiral sensors. The chiroptical properties of the molecules are usually characterized with circular dichroism (CD) and circularly polarized luminescence (CPL). CD describes the differential absorption of left- and right-handed circularly polarized light of the chirality of molecules in their ground states.¹ While CPL, the emission analog of CD, reveals the anisotropic emission of circularly polarized light of chiral luminescent systems in the excited state. Both methods provide conformational, and three-dimensional structural information of chiral materials.^{2,3} Functional materials with CPL properties have drawn

increasing attention recently for their promising applications as chemo/biosensors, optical information processing and storage devices.^{4,5} The performance of CPL-active materials is characterized with emission dissymmetry factor and luminescence efficiency. The emission dissymmetry factor (g_{em}), defined as $g_{em} = 2(I_L - I_R)/(I_L + I_R)$, where I_L and I_R are the emission intensities of the left- and right-handed circularly polarized light, respectively. The g_{em} values are in the range from -2 to $+2$ with the maximum absolute value of $g_{em} \sim 2$. To date, most of the reported CPL-active systems, such as lanthanide ion complexes,⁶ organic molecules,^{7,8} synthetic polymers,⁹⁻¹¹ have been investigated in their dilute solutions, and they show their absolute g_{em} values in the range of 10^{-5} – 10^{-2} . In condensed state, their CPL performance usually becomes worse because of aggregation caused quenching (ACQ) of luminescent molecules. Considering that CPL-active materials are inevitably employed in the form of thin film or bulk solids for practical use, designing of new chiral luminophores is thus highly demanded to meet the requirement of both high dissymmetry factors and emission efficiency in condensed phase.

Hybridization of chirality with organic π -conjugated molecules are usually used for the construction of CPL-active materials due to their structural diversity, synthetic feasibility, high flexibility and good processability. Apart from the prototype CPL-active luminophores based on some π -conjugated molecules including helicenes,¹²⁻¹⁴ and chiral bichromophores,^{15,16} a common strategy for the generation of CPL-active systems is to synthesize chiral luminescent molecules with planar luminophores in the core and chiral groups at the peripheries (Fig. 1a). Driven by the π - π stacking interactions, the chiral luminescent molecules self-assemble into helical architectures, which may generate CPL signals upon photo- or electro-excitation. However, conventional planar luminophores, such as pyrene and 3,4,9,10-perylenetetracarboxylic diimide, usually suffer from the notorious ACQ effect, that is they emit intensively in their dilute solutions, but become weakly fluorescent or non-emissive in aggregate and solid state.¹⁷ The ACQ effect greatly limits the application of planar luminophores in the construction of efficient CPL-active materials. In 2001, our group discovered that a group of propeller-shaped molecules showed a unique phenomenon of aggregation-induced emission (AIE), which was exactly contrary to ACQ effect.¹⁸ The AIE luminogens (AIEgens), such as silole, tetraphenylethene (TPE), are weakly or non-emissive in solutions, but emit intensively upon aggregation or in film state.¹⁹⁻²⁴ Based on experimental and theoretical studies, we have proposed a principle of restriction of intramolecular motions (RIM) including rotation and vibration of the molecules to explain the AIE phenomenon.²⁵ In solution, the dynamic molecular motions of AIEgens act as a relaxation channel for the energy of the excited state to decay nonradiatively, making the molecules non-emissive. Whereas in aggregated state, these motions are readily suppressed, which thus blocks the non-radiative decay channels and turns on their fluorescence. The discovery of the novel AIE molecules have paved a new avenue for the construction of efficient CPL-active materials, in particular for the application in condensed state. By appropriately integrating chiral moieties with AIE luminophores (Fig. 1b),²⁶ a series of AIE-based CPL materials have been developed, which have both large luminescence dissymmetry factors and high emission efficiency.²⁷

In this work, we summarize our work in the field of AIE-based CPL luminogens. We also describe the molecular design, AIE, CD, CPL, and helical self-assembly as well as the representative examples of chiral AIEgens.

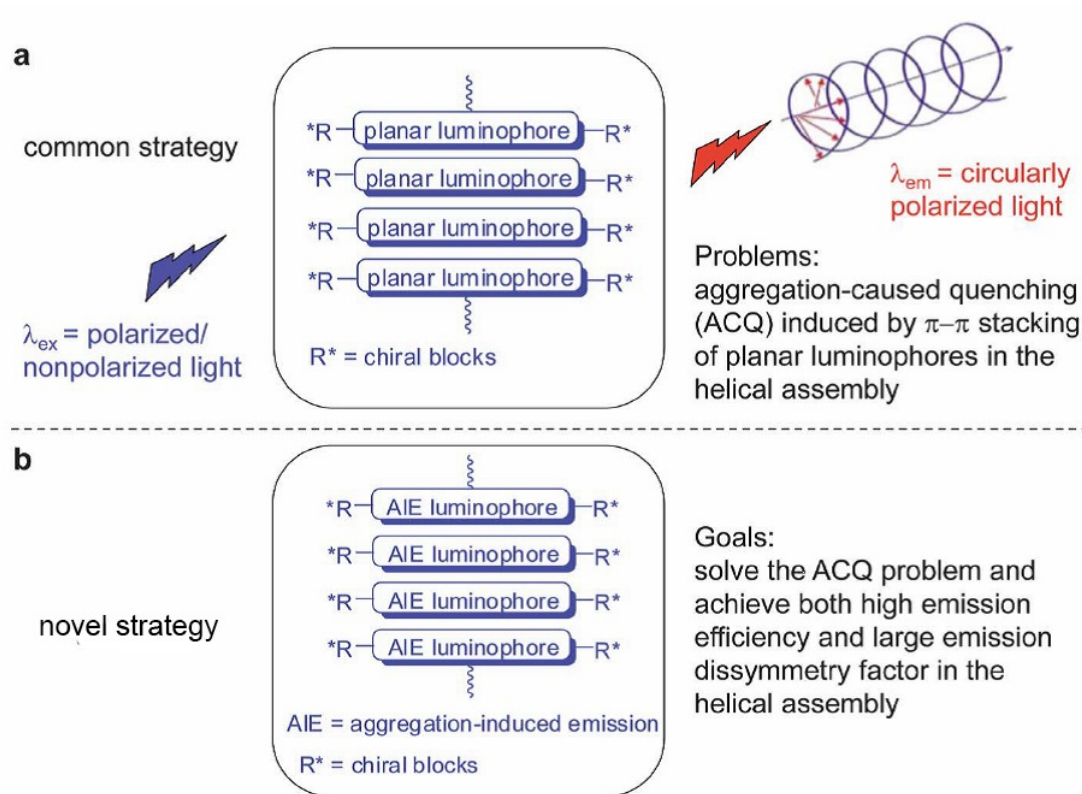


Fig. 1 Comparison of molecular design strategies to prepare CPL-active materials. CPL (output λ_{em}) is generated from helical assemblies of chiral luminescent molecules bearing (a) conventional planar and (b) AIE luminophores under the excitation of polarized/nonpolarized light (input λ_{ex}). Reprinted with permission from ref 26.

2 MOLECULAR DESIGN

In the generation of CPL-active materials with good performance in condensed state, high emission efficiency and CD absorption are prerequisite. Our strategy for the molecular design is to introduce chiral pendants into the periphery of AIEgens to guide the AIEgens to take chiral arrangements, as shown in Fig. 1b. We have chosen the archetypal AIEgens, silole and TPE, as the luminophores, and the naturally existing sugars, amino acids and binaphthol as the chiral pendants to fabricate CPL-active materials (Chart 1 and 2).

2.1 Silole derivatives

Siloles are a class of silicon-containing five-membered cyclic dienes. They are considered as a new kind of $\sigma^*-\pi^*$ conjugated materials with low-lying LUMO energy levels, resulting from the effective interaction between the σ^* orbital of the exocyclic silicon-carbon bond and the π^* orbital of the butadiene moiety.²⁸ Since the first report on the AIE phenomenon of a silole compound, 1-methyl-1,2,3,4,5-pentaphenylsilole, a lot of silole-based AIEgens with multiple functionalities and versatile applications have been designed and synthesized.^{29,30} On the other hand, saccharides and

amino acids are naturally occurring chiral molecules. It is anticipated that modification of AIEgens with chiral saccharide or amino acid groups will generate CPL-active materials.

We first chose tetraphenylsilole derivative as the luminophore and mannose as the chiral building block, and synthesized **1** through Cu(I)-catalyzed azide-alkyne “click” reaction.²⁶ Using the same luminophore and synthetic route, we then prepared another chiral silole derivatives **2** and **3** carrying L-valine- and L-leucine attachments, respectively.^{31,32} To expand the molecular system, we also synthesized chiral silole derivative **4** with chiral phenylethanamine moieties using thiourea as linkers.³³

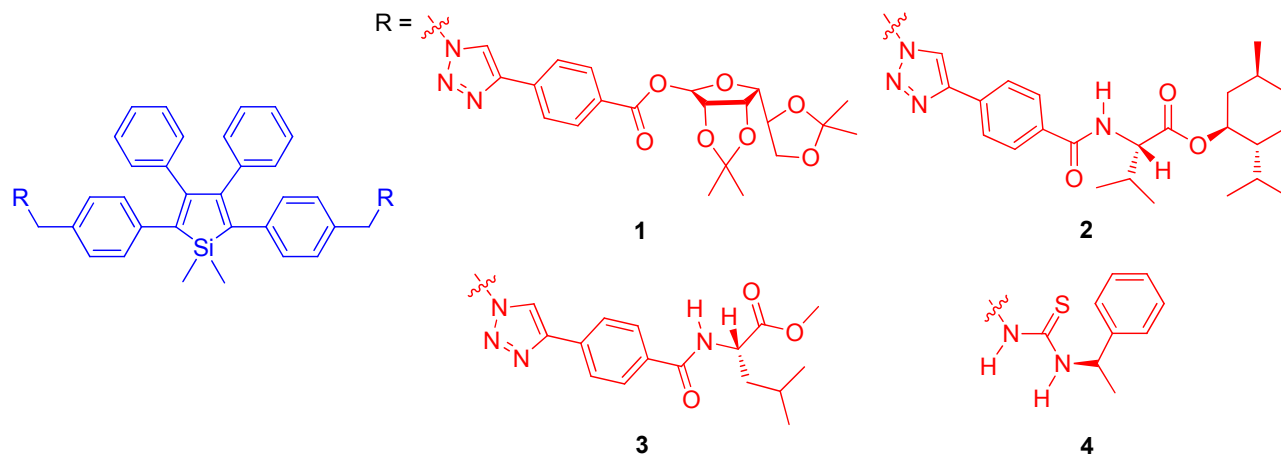


Chart 1. The chemical structures of chiral silole derivatives 1–4.

2.2 TPE derivatives

Despite the high quantum yields, silole derivatives require complicated synthesis steps that involves reactive organometallic species and sensitive intermediates. Moreover, the silole rings become unstable under basic conditions, which restrict their applications. With respect to this respect, TPE derivatives have facile synthesis, easy functionalization and good stability and thus are alternative AIE luminophores for constructing CPL materials.

TPE derivatives have chiral arrangements in their crystal form,³⁴ but under conventional condition they usually exist as racemers or mesomers and barely have chiroptical property. To enhance their chiroptical property, chiral pendants need to be brought to the TPE scaffolds to induce them to have chiral arrangement. By introducing L-valine- and L-leucine-containing attachments to TPE scaffolds, mono-substituted chiral TPE derivatives **5** and **6**, and two substituted chiral TPE derivative **7** containing bivaline attachments were synthesized. These derivatives provide important insight of the influence of the types and number of chiral substituents on the CPL properties and self-assembly behaviors of chiral AIE derivatives.³⁷ Besides AIEgens with -point chirality, AIEgens **8–10** with axial chirality were synthesized by welding TPE units with an axial chiral moiety, binaphthol.³⁸

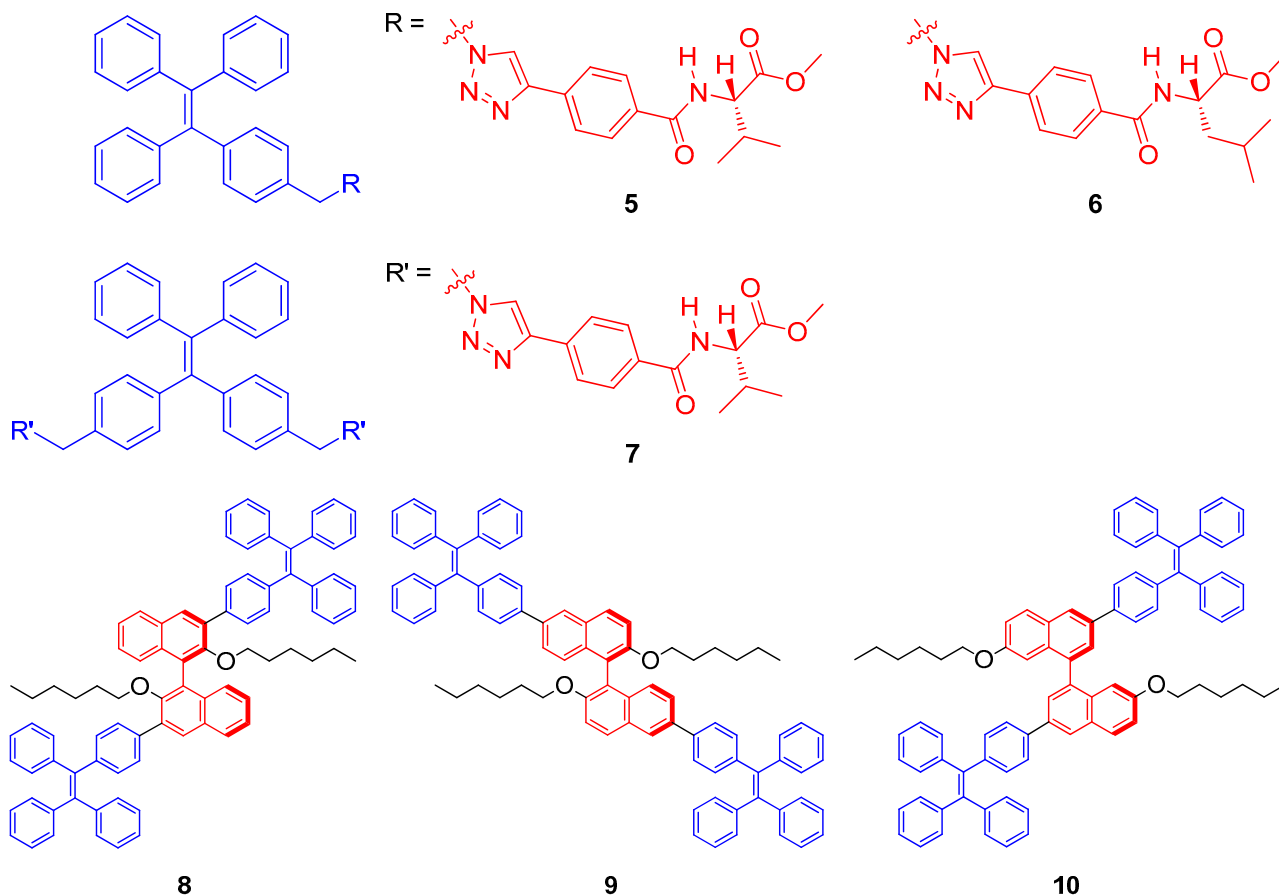


Chart 2. The chemical structures of chiral TPE derivatives 5–10.

3 AGGREGATION-INDUCED EMISSION

Compounds 1–10 are all AIE-active. As exemplified with 1, it is nearly non-emissive in its dichloromethane (DCM) solution and DCM–hexane mixtures with hexane fractions lower than 80%, but it emits intensively upon the addition of more poor solvent (Fig. 1a). The changes of its fluorescence quantum yields (Φ_F) further confirm its AIE activity. Its Φ_F is about 0.6% in DCM solution, but increases to 31.5% in the DCM–hexane mixture and reaches 81.3% at film state (Fig. 1b).

To reveal the underlying mechanism of AIE phenomenon, we further investigated the dynamics of emission of 1 by measuring fluorescence lifetime and the influence of the low-frequency motions on the fluorescence efficiency through theoretical calculations. Both experimental and theoretical results are in accordance with our proposed a RIM principle. When 1 is molecularly dissolved in solution, its low frequency intramolecular motions annihilate the excitons in a non-radiative way, making it weakly or non-emissive; whereas in the aggregate state, the intramolecular motions are greatly restricted, thus blocking the nonradiative energy decay and leading to the light emission.

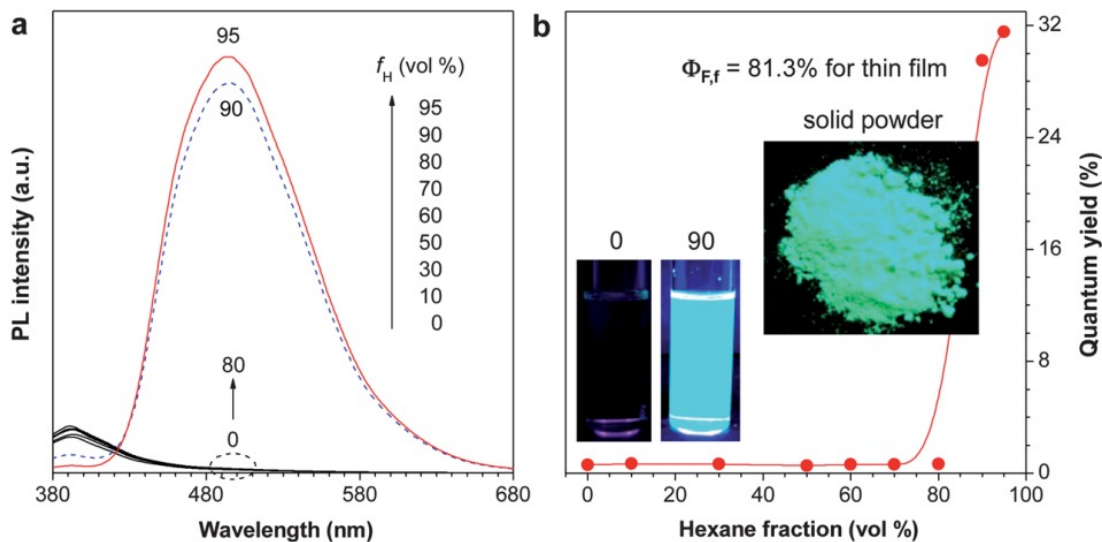


Fig. 2 (a) Photoluminescence (PL) spectra of **1** in dichloromethane (DCM) with different volume fractions of hexane (f_H) (Concentration: 10^{-5} M, λ_{ex} : 356 nm). (b) Variation of fluorescence quantum yields (Φ_F) of **1** versus f_H of the DCM-hexane mixture; the insets show the fluorescent photographs of **1** in DCM and DCM-hexane with f_H of 90% and its powder under irradiation with a hand-held UV-lamp (365 nm). Reprinted with permission from ref 26.

4 CIRCULAR DICHROISM

CD provides the specific chiroptical information of molecules in the ground state. It is quantified by using the absorptive dissymmetry factor, which is defined as $g_{\text{abs}} = 2(\epsilon_L - \epsilon_R)/(\epsilon_L + \epsilon_R)$, where ϵ_L and ϵ_R are the molar extinction coefficients of the left- and right-handed circularly polarized light, respectively.

The AIEgens **1–3** and **5–7** with chiral substituents are all CD-silent in their dilute solutions, but give strong CD signals in the aggregate and solid state, showing aggregation-induced CD (AICD). As exemplified with the absorption and CD spectra of molecule **1**, it exhibits two absorption peaks at the wavelengths of 279 and 360 nm in DCM solution (Fig. 3a), which correspond to the absorptions of the peripheral triazolylphenyl groups and the silole core, respectively; In DCM solutions with different concentrations, the CD spectra of **1** give no CD signals (Fig. 3b), whereas in DCM-hexane mixture (1/9, v/v), they show Cotton effects at the wavelength of 249, 278 and 340 nm, and the intensities increase with an increase in the concentration (Fig. 3c), exhibiting an AICD effect. The peaks at the wavelength of 278 and 249 nm are assigned to the absorptions of the triazolylphenyl moiety, while the peaks at 340 nm is attributed to the absorption of the π - π conjugated system of the silole. It indicates that the chirality has been transferred from the sugar-containing attachments to the silole core in the aggregate state. Additionally, the g_{abs} values at 360 nm are increased from 1.59 to 2.23×10^{-3} with the concentration from 2×10^{-5} to 2×10^{-4} . The AICD effect is further proved by the CD spectra of thin solid film of **1** dispersed in poly(methyl methacrylate) (PMMA) matrix with different weight fractions (wt%). At 2.5 wt%, no CD signals are observed. At higher wt%, CD signals occur and the intensities increase with an increase in the loading amount (Fig. 3d). Furthermore, a more significant red shift occurs in film state than that in DCM/hexane mixture, which may be caused by the formation of more conjugated helical structures.

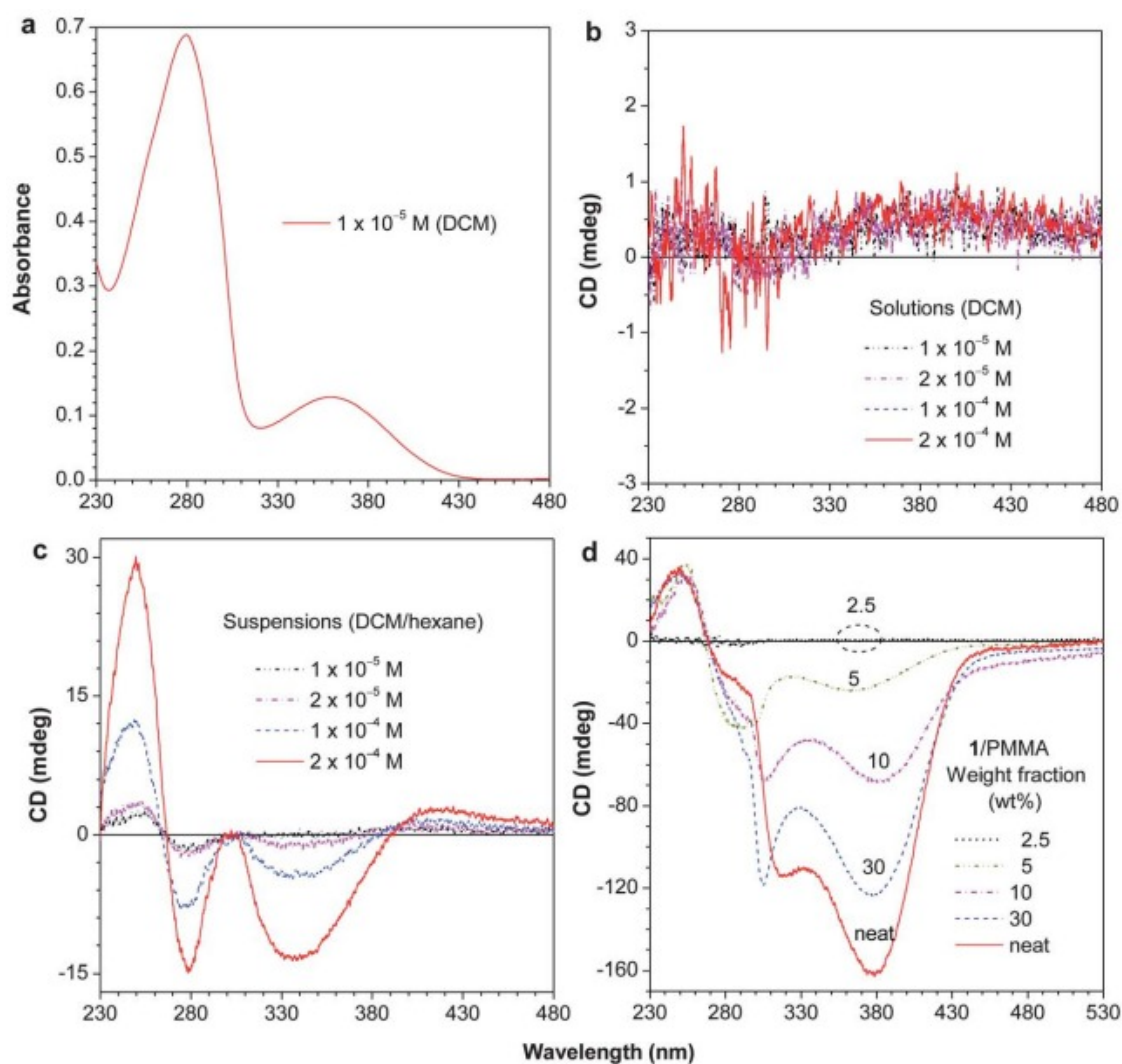


Fig. 3 (a) Absorption spectrum of **1** in DCM. (b) and (c) CD spectra of **1** with different concentrations in DCM solution and DCM/hexane (1/9, v/v) mixtures, respectively. (d) CD spectra of **1** with different weight fractions (wt%) dispersed in PMMA matrix prepared by drop casting of their mixed 1,2-dichloroethane (DCE) solutions. Concentration of PMMA : 10 mg mL⁻¹. CD spectrum of neat **1** prepared by natural evaporation of its DCE solution of 2 mg · mL⁻¹ on a quartz plate is also shown for comparison. Reprinted with permission from ref 26.

Interestingly, the silole derivative **4** with thiourea linkages and chiral phenylethanamine pendants shows a complexation-induced CD (CICD) effect.³³ When it is molecularly dissolved in good solvent or upon the addition of poor solvents, no CD signals are observed. But when complexed with chiral acids, such as mandelic acids and phenyllactic acids, **4** becomes CD-active in the thin film (Fig. 4), indicating that the complexation between the thiourea groups and the chiral acids efficiently induces the chirality transfer. It was found that such a CICD effect was the most effective in the complexation of **4** with mandelic acid due to their structural features.

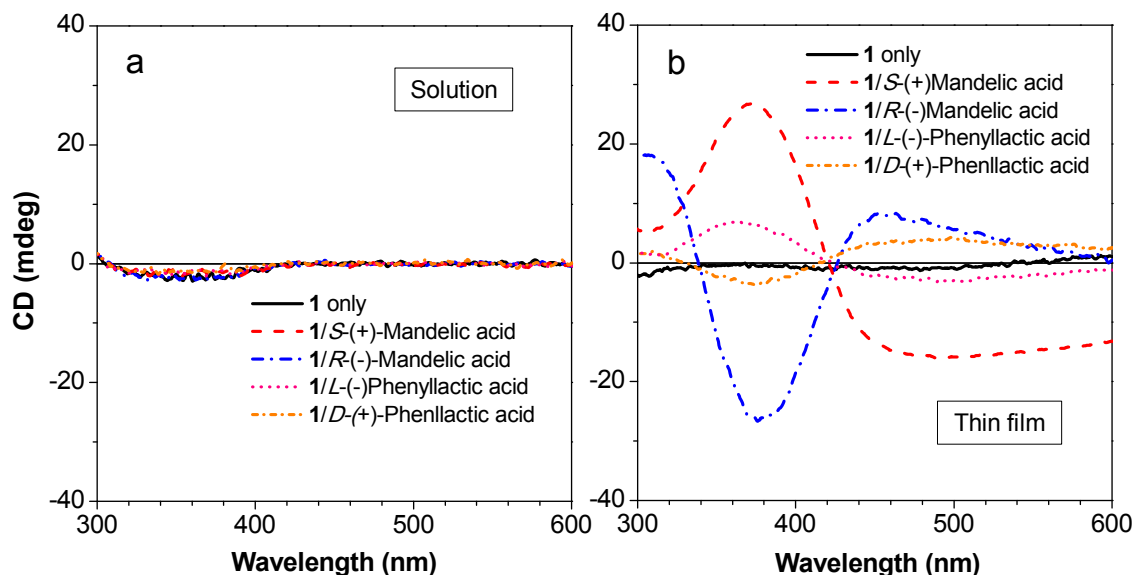


Fig. 4 CD spectra of **4** in the absence and presence of chiral hydroxyl acids in (a) THF solution and (b) solid thin film states. Concentration of **4** : 1 mM; Concentration of acid: 40 mM. Reprinted with permission from ref 33.

Unlike the AIEgens with point chirality, the AIEgens **8–10** with axial chirality show an abnormal phenomenon of aggregation-annihilation CD (AACD). The CD signals of the AIEgens remained unchanged in THF/water mixtures with water fractions (f_w) lower than 40%, but decreased when f_w is higher than 40% (Fig. 5). A series of control experiments suggest that the AACD effect is likely caused by the decrease of twisted angle between two naphthalene rings in these AIEgens.³⁸

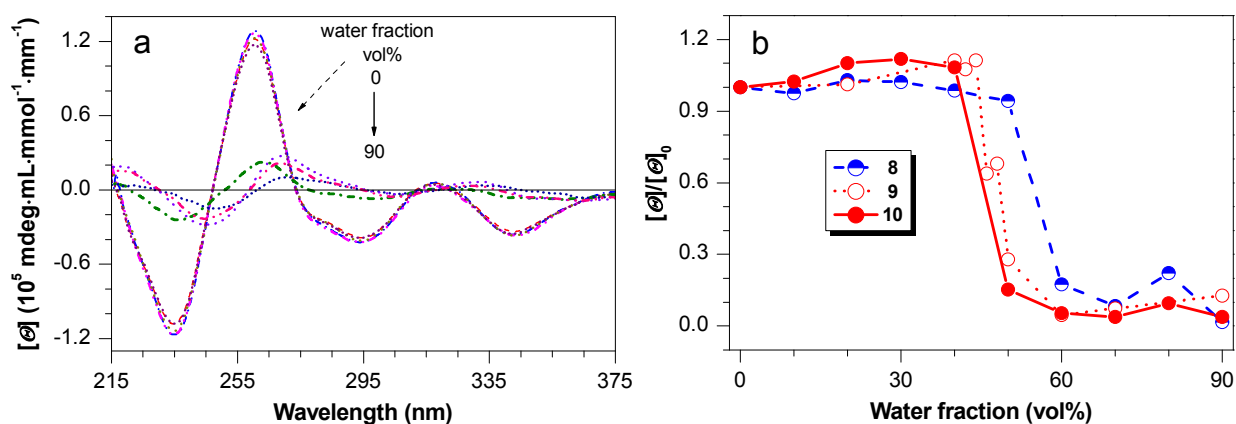


Fig. 5 (a) CD spectra of **8** in THF/water mixtures with different water fractions (f_w). Concentration : 10^{-4} M. (b) Plots of relative molar ellipticity of **8** (@ 260 nm), **9** (@280 nm), and **10** (@280 nm) versus f_w . $[\theta]$ = molar ellipticity, $[\theta]_0$ = molar ellipticity at $f_w = 0$. Reprinted with permission from ref 38.

5 CIRCULAR-POLARIZED LUMINESCENCE

Since the AIEgens **1–7** are both highly emissive and CD-active in aggregate state, they are anticipated to have CPL properties. This is the case. In this part, we mainly focus on the sugar-containing silole derivative **1**.

The CPL behaviors of **1** are explored at various sample forms, including solution, suspended particles, cast film, dispersion in PMMA matrix and micropatterned film prepared by using microfluidic technique.³⁹ Images of fluorescence microscope at these conditions are captured, as shown in Fig. 6a-6f. Molecule **1** doesn't give any CPL signals in solution, because it is non-emissive and CD-silent, whereas in the aggregate state, it gives obvious negative CPL signals, showing an aggregation-induced CPL (AICPL) effect as shown in Fig. 6g and 6h. This indicates that predominant one-handed helical structures are formed in the aggregates. The CPL spectra in the aggregate state have similar profiles, but diverse g_{em} values. In DCM/hexane (v/v, 1/9) mixture, cast film obtained by evaporating its DCE solution, and doped PMMA film, the g_{em} values of **1** are in the range of -0.17 to -0.08 and show less dependence on the emission wavelength. Surprisingly, the g_{em} value of **1** can reach up to -0.32 in the fabricated pattern prepared by allowing the evaporation of its DCM/toluene solution in Teflon-based microchannels. To the best of our knowledge, the value is the highest record for organic chiral π -conjugated molecules. This high g_{em} may be caused by the improved coverage and packing order of the molecules in the confined microchannel environment. The variation in the g_{em} values of **1** in different forms suggests that supramolecular structures play an important role in determining the CPL activities. Molecule **1** also has good spectral stability that it still remains CPL after more than half a year storage under ambient conditions. This CPL system thus represents the best result in the organic chiral conjugated materials meeting the requirement of both high luminescence efficiency and dissymmetry factor.

Using the same micropatterning method, we also fabricated micropatterns of the valine-containing TPE derivative **5** for CPL measurement. It gives positive signals and an average g_{em} value of 0.03 in the wavelength range of $400\text{--}600$ nm, showing less dependence on the emission wavelength (Fig. 7). Similar to **1** and **5**, the chiral amino acid-containing AIEgens **2**, **3**, **6** and **7** are all CPL-active in solid thin film state and show their average g_{em} values about -0.05 , -0.016 , 0.045 and -0.003 , respectively,^{31,32,37,38} which are comparable to those ($|g_{em}| = 10^{-5}\text{--}10^{-2}$) of most reported organic functional materials with CPL activities.^{7,8} Such results further prove that hybridization of chiral pendants with AIEgens is an efficient molecular design strategy for the construction of CPL-active materials in condensed phase. This kind of materials are certainly promising candidates for high-tech applications in term of their high emission efficiency and g_{em} values in solid state.

In contrast to the chiral AIEgens described above, the solid thin film of **4** alone gives nearly no CPL signals, suggesting that its conformation is randomly arranged. When complexed with R(-)-mandelic acid and S(+)-mandelic acid, the solid film of **4** shows the average g_{em} values about -0.01 (Fig. 8a) and $+0.01$ (Fig. 8b), respectively, demonstrating a complexation-induced CPL effect. Furthermore, the CPL signal of **4** can be tuned inversely by complexation with either enantiomer of mandelic acids. Due to the AACD effect, the chiral AIEgens **8–10** exhibit very weak CPL signals in the condensed phase.

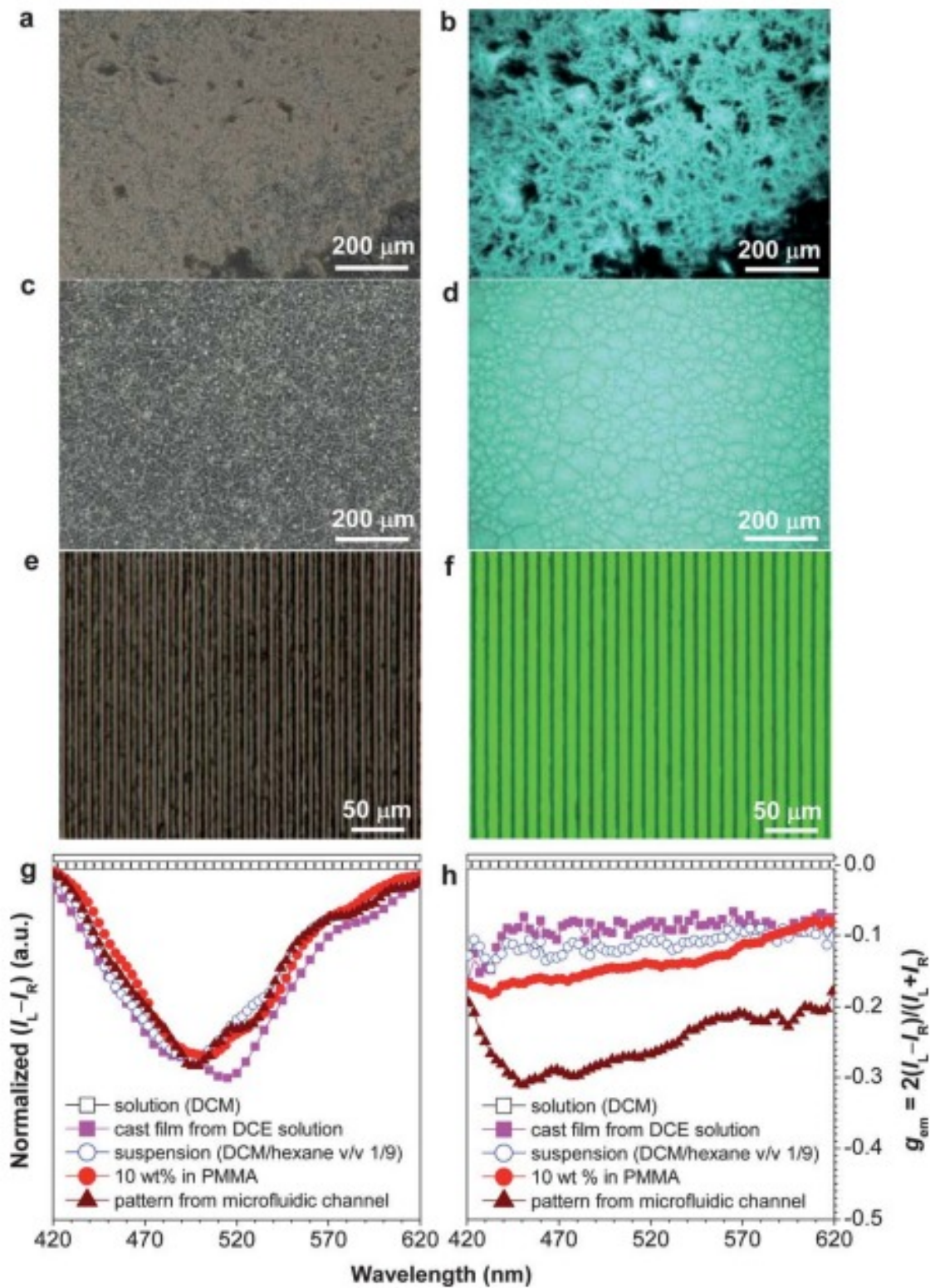


Fig. 6 (a–f) Images Fluorescence microscope under normal laboratory lighting (left panels) and UV excitation (right panels) of **1**: (a and b) natural evaporation of DCE solution, (c and d) dispersion in PMMA matrix (10 wt%), and (e and f) evaporation of

DCM–toluene solution in microfluidic channels on quartz substrates. (g and h) Plots of (g) ($I_L - I_R$) and (h) CPL dissymmetry factor g_{em} versus wavelength for **1** existing in different formats: DCM solution, DCM–hexane (v/v, 1/9) mixture (suspension), neat cast film from DCE solution of 2 mg mL^{-1} , dispersion in polymer matrix (10 wt% in PMMA), and fabricated micropattern by evaporating of DCE solution in microfluidic channels. In DCM and DCM–hexane mixture, concentration: $2 \times 10^{-4} \text{ M}$, λ_{ex} : 356 nm. Reprinted with permission from ref 26.

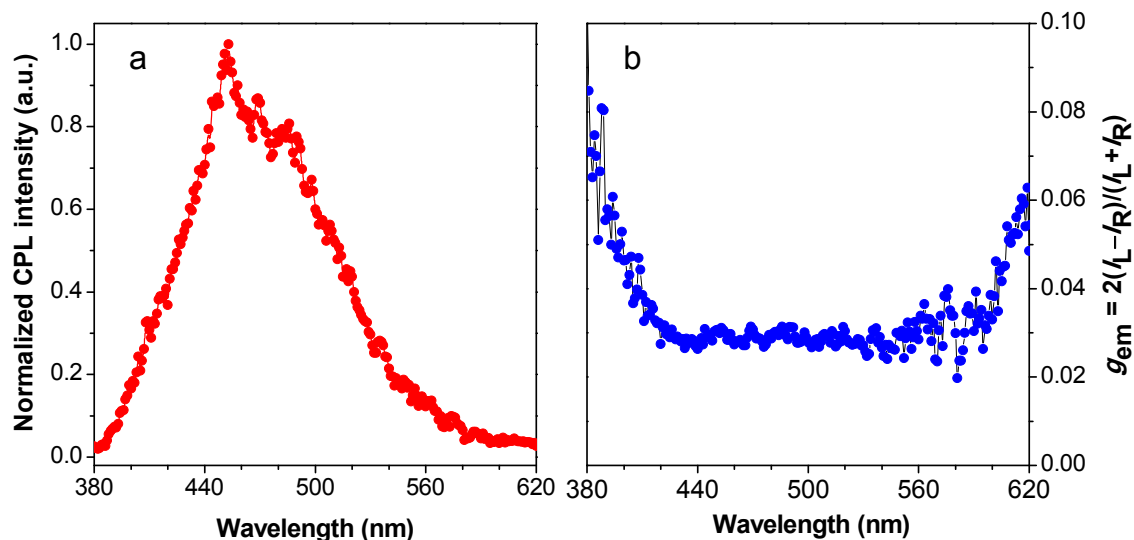


Fig. 7 Plots of (a) CPL and (b) CPL dissymmetry factor (g_{em}) versus wavelength of micropatterns formed by **5**, λ_{ex} : 325 nm. Reprinted with permission from ref 35.

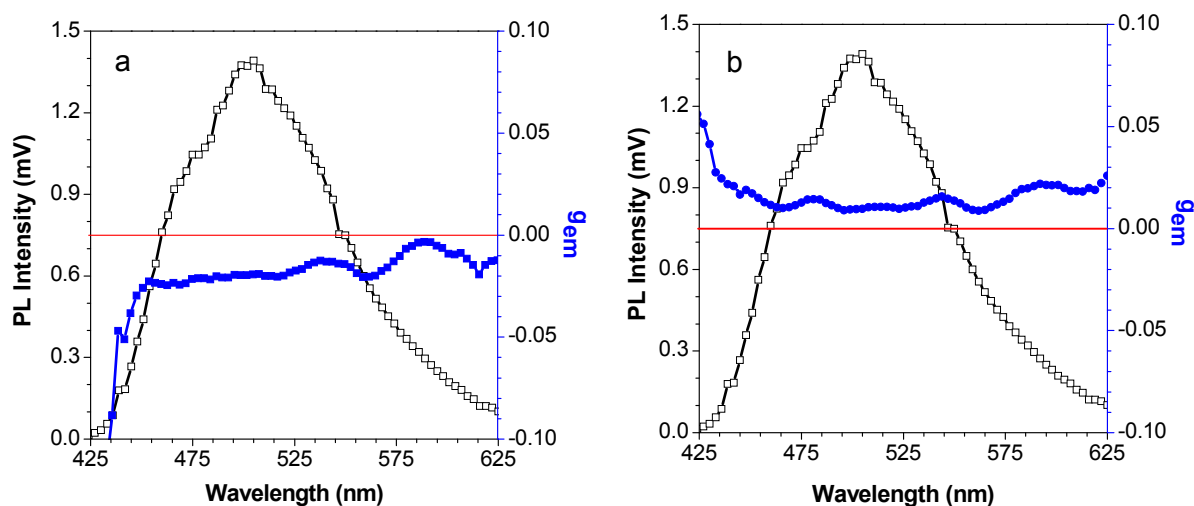


Fig. 8 Plots of PL intensity and g_{em} versus wavelength for **4** in the presence of (a) R-(–) or (b) S-(+)-mandelic acid ($[4]/[\text{acid}] = 1 : 40$ by mole) in the film state, respectively. Reprinted with permission from ref 33.

6 SELF-ASSEMBLY

Self-assembly is the spontaneous formation of ordered structures from disordered components via specific noncovalent interactions such as van der Waals, π - π , and hydrogen-bonding interactions. The AICD and AICPL effects of the chiral AIEgens imply that predominantly one-handed helical structures are formed in the aggregate states. We thus investigated their self-assembly behaviors by using the microscopy techniques. As shown in Fig. 9, molecule **1** self-assembles into preferred right-handed helical nanoribbons upon aggregation in DCM–hexane mixture (90% volume ratio of hexane), and evaporation of its DCE solution. The average width and helical pitch of the formed nanoribbons are about 30 and 120–150 nm, and their length can be up to micrometers. Through using powder X-ray diffraction (XRD) technique and structural simulation, we consider that the driving force for the self-assembly process comes from a cooperative effect of the multiple noncovalent interactions, such as weak hydrogen bonding interactions (C–H \cdots O and C–H \cdots N), π - π stacking, and stereo-shaped complementary between the sugar-containing pendants.

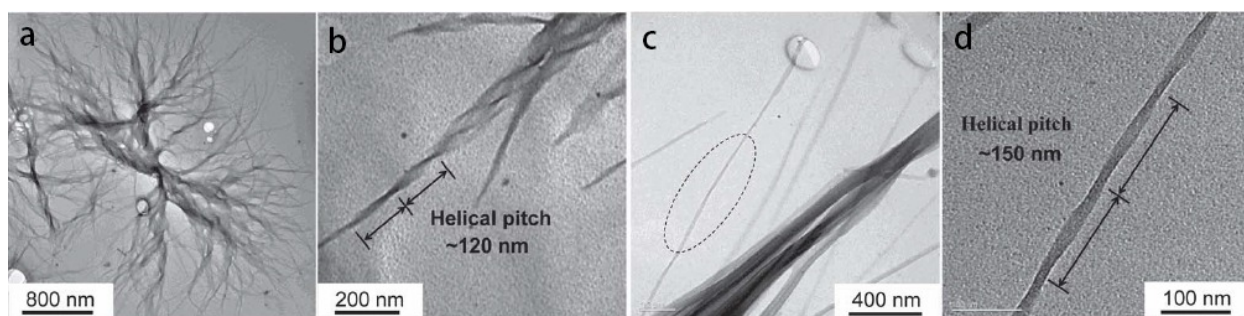


Fig. 9 (a–d) TEM images of the aggregates of **1** (a and b) in DCM/hexane mixture (1/9, v/v), (c) from natural evaporation of DCE solution of 2 mg mL⁻¹, and (d) enlarged area circled in panel c. Reprinted with permission from ref 26.

The morphologies of the aggregates of **2** were examined by AFM. As shown in Fig. 10a, helical nanofibers with consistent left-handedness were generated by **2** on the evaporation of its THF solution. Chiral aggregates were also formed on the addition of a poor solvent, such as water and hexane, into its THF solution. With increasing the water content, the morphologies of the aggregates of **2** transformed from extended helical fibers to loops (Fig. 10b) and finally to the network of fibers (Fig. 10c), which all show left handedness. When 10% volume ratio of hexane added into the THF solution of **2**, it was found that the previous formed helical fiber structures converted into networked structures (Fig. 11a). Braids of fibers arranged in a nebular-like morphology were obtained with increasing hexane content to 50% volume ratio (Fig. 11b). Interestingly, right-handed helical fibers were generated by adding 80% volume ratio of hexane (Fig. 11c), indicative of an inversion in the handedness of the formed helical fibers. We also investigated the self-assembly behaviors of **3** by using AFM and SEM. It was found that it could readily form left-handed helical fibers upon evaporation of its DCE solution and DCE–hexane mixtures with different fractions of hexane.

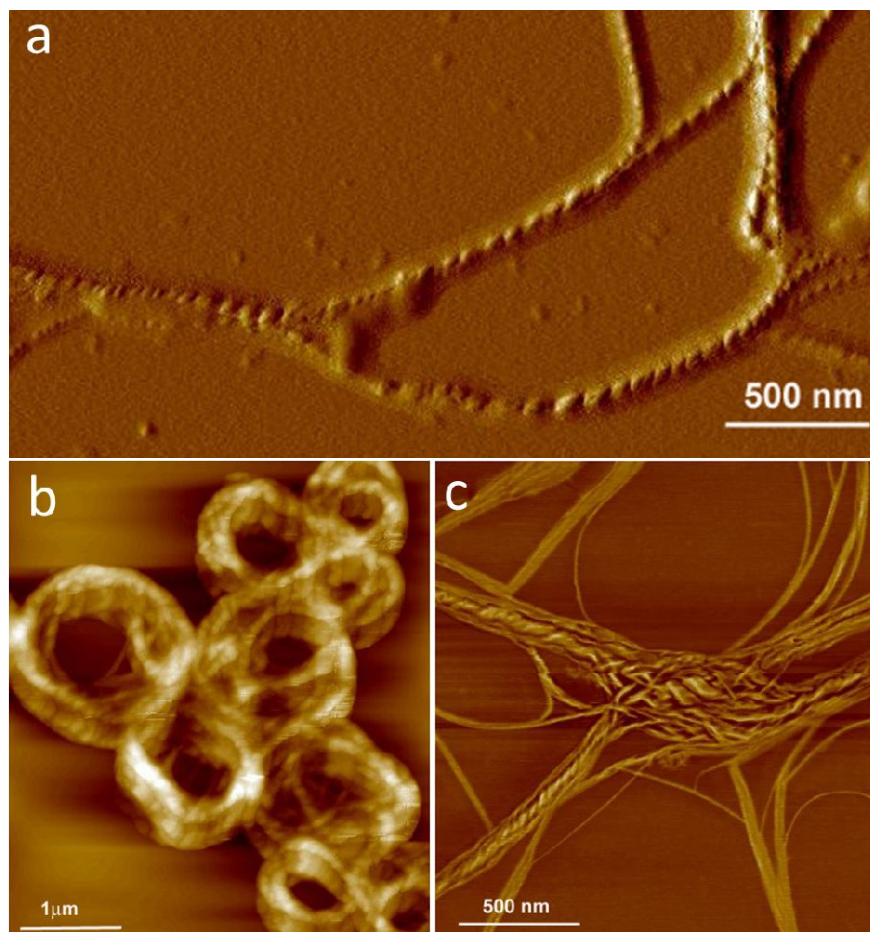


Fig. 10 AFM images of helical assemblies formed by **2** upon evaporation of its THF solution (a) and THF–water mixtures with water fractions of 20 vol % (b) and 90 vol % (c). Reprinted with permission from ref 31.

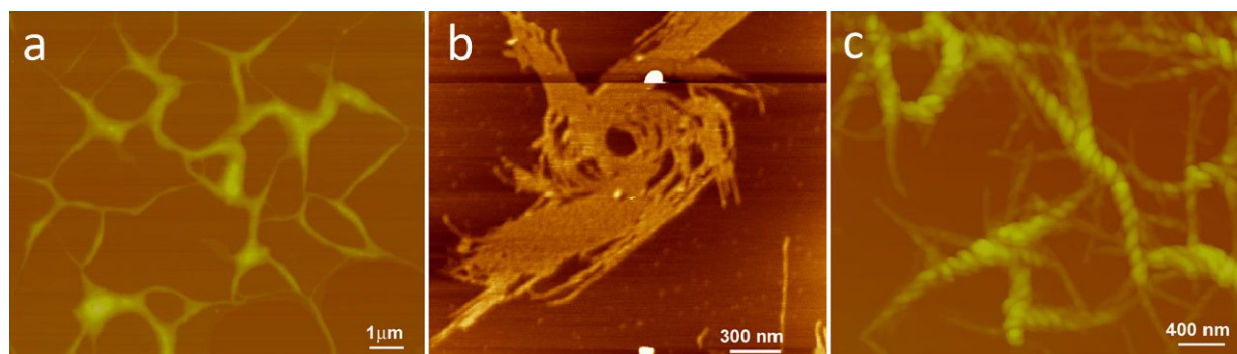


Fig. 11 AFM images of the manipulated assemblies formed by **2** upon evaporation of its different THF–hexane mixtures with hexane volume fractions of 10% (a), 50 % (b), 80 % (c). Reprinted with permission from ref 31.

Besides the chiral silole derivatives, the TPE-based chiral AIEgens **5–7** can also assemble into helical structures. As shown in Fig. 12, monofunctionalized TPE derivatives **5** and **6** carrying either L-valine- or L-leucine-containing

attachment readily self-assemble into left-handed helical fibers and ribbons by evaporation of their DCE–hexane mixtures (1/9, v/v). The individual helical fibers can further twine to form multi-stranded helices with left-handedness and several micrometers lengths (Fig. 12a). Fig.12b and 12c show co-existence of helical fiber, ribbons, and combined structures, which indicates that helical fibers are likely wrapped up by the ribbons. The fluorescence microscopy image of **6** exhibits that the fibers with lengths of up to millimeters and intense blue fluorescence (Fig. 12d), further proving their strong self-assembly activities. We then investigated the influence of the number of chiral substituents on the self-assembly behaviors of TPE-based chiral AIEgens. It was found that chiral TPE derivative **7** bearing two L-valine attachments can readily form helical fibers with consistent right-handedness in DCE solution upon solvent evaporation (Fig.13). The results of XRD and computational simulation demonstrate a synergistic effect from multiple intermolecular hydrogen bonding interactions, π - π interactions, and the steric effect between the attachments may serve as the driving force for the assembling process.

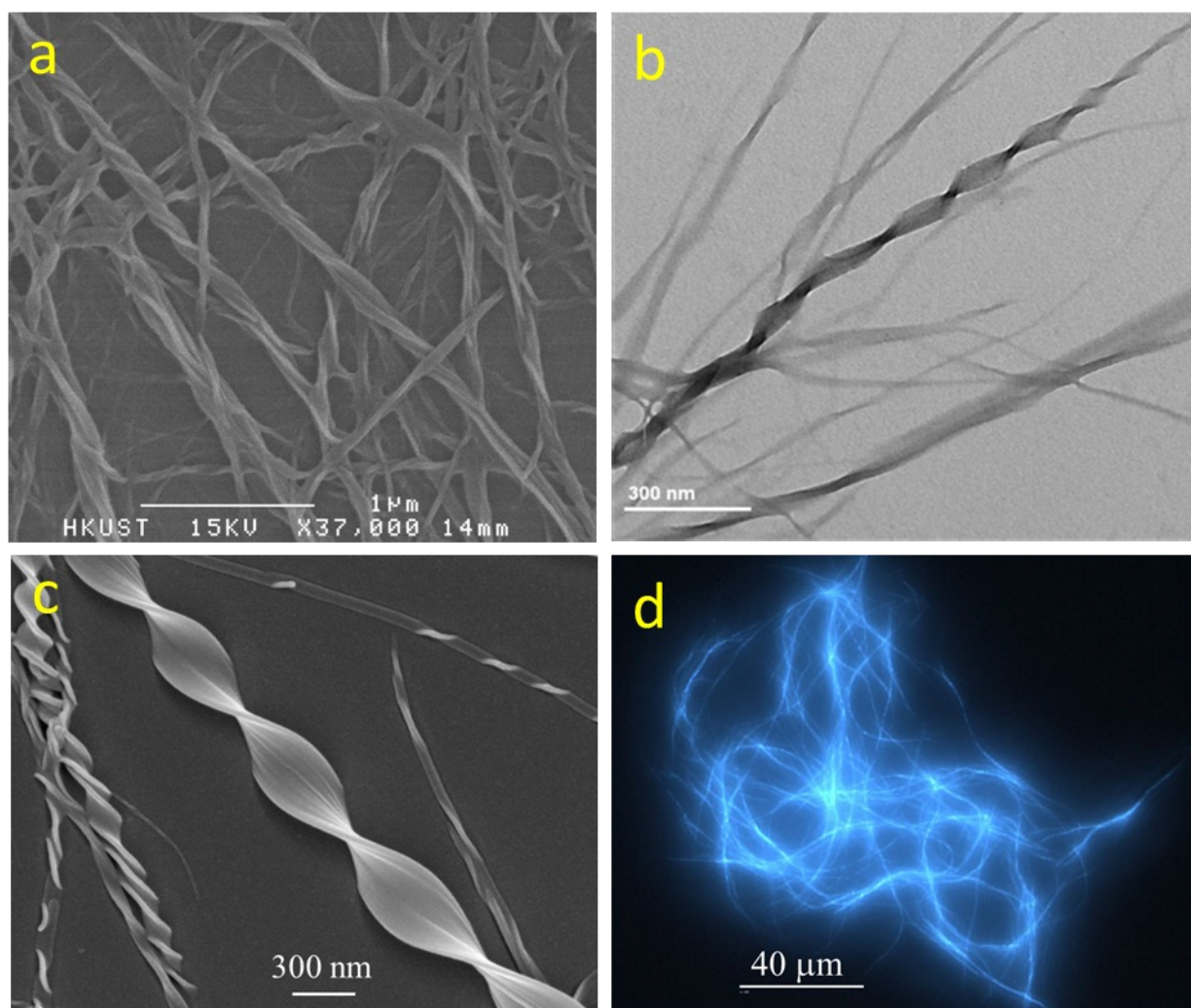


Fig. 12 SEM (a) and TEM (b) images of the aggregates of **5** formed upon the evaporation of DCE–hexane solution (1/9, v/v), $[5] = 10^{-4}$ M. Reprinted with permission from ref 35. SEM (a) and fluorescence microscopy (b) images of the aggregates of **6** formed upon the evaporation of DCE–hexane solution (1/9, v/v), $[6] = 10^{-4}$ M. Reprinted with permission from ref 36.

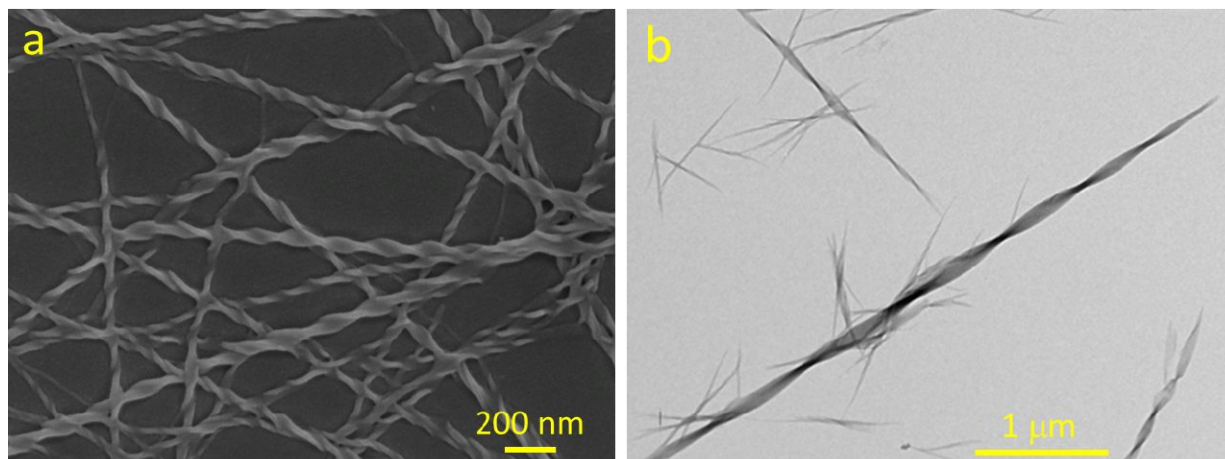


Fig. 13 SEM (a) and TEM (b) images of **7** formed by natural evaporation of its DCE solution, $[7] = 10^{-4}$ M. Reprinted with permission from ref 37.

7 CONCLUSIONS

In this review, we have summarized our work in molecular design, CPL property and self-assembling behaviors of chiral AIEgens due to the space limitation. The discovery of AIEgens provides a new strategy for solving ACQ effect. This unique luminescence property of AIE makes AIEgens the promising scaffolds for the construction of efficient CPL-active materials in condensed phase. By introducing chiral elements into AIE luminophores, a group of chiral AIEgens with *-point* and axial chirality are designed and synthesized. They all display high emission efficiency and good CPL performance in the solid state. Molecule **1**, gives the highest CPL dissymmetry factor of -0.32 , a record for organic CPL materials. These chiral AIEgens also have the ability to self-assemble into fluorescent helical fibers and ribbons with predominantly one-handedness.

Hybridization of chirality with AIEgens is a feasible strategy for the construction of AIE-based CPL luminogens. These kinds of molecules with excellent CPL performance are novel functional materials for the utility in the area of chiral sensing and possessing in particular for the condensed phase. Fabricating AIE-based CPL luminogens into micro/nanostructures further paves their way in a more broad application field of miniaturized optoelectronic devices. In this regard, more knowledge is still needed for revealing the intermolecular interactions and structure control. Further efforts should focus on the underlying mechanism of the cooperative effect of chirality and AIE in order for better function development.

ACKNOWLEDGMENTS

This work was partially supported by the National Science Foundation of China (21104046, 21404077 and 21574085), the Outstanding Youth Foundation of Shenzhen (JC201005250038A, JCYJ20140509172609153), the National Basic Research Program of China (973 program, 2013CB834701), the Research Grants Council of Hong Kong (604711, 604913 and N_HKUST620/11) and the University Grants Committee of Hong Kong (AoE/P-03/08).

REFERENCES

- (1) K. Nakanishi, N. Berova, and R. W. Woody, *Circular Dichroism, Principles and Applications*, VCH Publishers, New York (1994).
- (2) F. S. Richardson and J. P. Riehl, "Circularly polarized luminescence spectroscopy," *Chem. Rev.* **77**(6), 773–792 (1977).
- (3) J. P. Riehl, "Circularly polarized luminescence spectroscopy," *Chem. Rev.* **86**(1), 1–16 (1986).
- (4) H. Maeda et al., "Chemical-stimuli-controllable circularly polarized luminescence from anion-responsive π -conjugated molecules," *J. Am. Chem. Soc.* **133**(24), 9266–9269 (2011).
- (5) C. Wagenknecht et al., "Experimental demonstration of a heralded entanglement source," *Nat. Photonics* **4**, 549–552 (2010).
- (6) F. Zinna and L. D. Bari, "Lanthanide circularly polarized luminescence: bases and applications," *Chirality* **27**(1), 1–13 (2015).
- (7) E. M. Sánchez-Carnerero et al., "Circularly polarized luminescence from simple organic molecules," *Chem. Eur. J.* **21** (39), 13488–13500 (2015).
- (8) J. Kumar, T. Nakashima, and T. Kawai, "Circularly polarized luminescence in chiral molecules and supramolecular assemblies," *J. Phys. Chem. Lett.* **6**(17), 3445–3452 (2015).
- (9) B. M. W. Langeveld-Voss et al., "Circular dichroism and circular polarization of photoluminescence of highly ordered poly{3,4-di[(S)-2-methylbutoxy]thiophene}," *J. Am. Chem. Soc.* **118**(20), 4908–4909 (1996).
- (10) S. Fukao and M. Fujiki, "Circularly polarized luminescence and circular dichroism from Si–Si-bonded network polymers," *Macromolecules* **42**(21), 8062–8067 (2009).
- (11) A. Satrijo, S. C. J. Meskers, and T. M. Swager, "Probing a conjugated polymer's transfer of organization-dependent properties from solutions to films," *J. Am. Chem. Soc.* **128** (28), 9030–9031 (2006).
- (12) Y. Sawada et al., "Rhodium-catalyzed enantioselective synthesis, crystal structures, and photophysical properties of helically chiral 1,1'-bitriphenylenes," *J. Am. Chem. Soc.* **134**(9), 4080–4083 (2012).
- (13) K. Goto et al., "Intermolecular oxidative annulation of 2-aminoanthracenes to diazaacenes and aza[7]helicenes," *Angew. Chem., Int. Ed.* **51**(41), 10333–10336 (2012).
- (14) K. Nakamura et al., "Enantioselective synthesis and enhanced circularly polarized luminescence of S-shaped double azahelicenes," *J. Am. Chem. Soc.* **136**(15), 5555–5558 (2014).
- (15) K. Nakabayashi et al., "Nonclassical dual control of circularly polarized luminescence modes of binaphthyl-pyrene organic fluorophores in fluidic and glassy media," *Chem. Commun.* **50**(87), 13228–13230 (2014).
- (16) T. Amako et al., "Pyrene magic: chiroptical enciphering and deciphering 1,3-dioxolane bearing two wirepullings to drive two remote pyrenes," *Chem. Commun.* **51**(39), 8237–8240 (2015).
- (17) J. B. Birks, *Photophysics of Aromatic Molecules*, Ed.; Wiley: London (1970).

- (18) J. Luo et al., "Aggregation-induced emission of 1-methyl-1,2,3,4,5- pentaphenylsilole," *Chem. Commun.* 1740–1741 (2001).
- (19) Y. Hong, J. W. Y. Lam, and B. Z. Tang, "Aggregation-induced emission: phenomenon, mechanism and applications," *Chem. Commun.* 4332–4353 (2009).
- (20) Y. Hong, J. W. Y. Lam, and B. Z. Tang, "Aggregation-induced emission," *Chem. Soc. Rev.* **40**(11), 5361–5388 (2011)
- (21) R. Hu, N. L. Leung, and B. Z. Tang, "AIE macromolecules: syntheses, structures and functionalities," *Chem. Soc. Rev.* **43**(13), 4494–4562 (2014).
- (22) R. T. K. Kwok et al., "Biosensing by luminogens with aggregation-induced emission characteristics," *Chem. Soc. Rev.* **44**(13), 4228–4238 (2015).
- (23) H. Wang et al., "AIE luminogens: emission brightened by aggregation," *Materials today* **18**(7), 365–377 (2015).
- (24) J. Mei et al., "Aggregation-induced emission: together we shine, united we soar!" *Chem. Rev.* **115**(21), 11718–11940 (2015).
- (25) J. Mei et al., "Aggregation-induced emission: the whole is more brilliant than the parts," *Adv. Mater.* **26**(31), 5429–5479 (2014).
- (26) J. Liu et al., "What makes efficient circularly polarised luminescence in the condensed phase: aggregation-induced circular dichroism and light emission," *Chem. Sci.* **3**(9), 2737–2747 (2012).
- (27) J. Roose, B. Z. Tang, and K. S. Wong, "Circularly-polarized luminescence (CPL) from chiral AIE molecules and macrostructures," *Small* DOI: 10.1002/sml.201601455 (2016).
- (28) C. Chuit et al., "Reactivity of penta- and hexacoordinate silicon compounds and their role as reaction intermediates," *Chem. Rev.* **93**(4), 1371–1448 (1993).
- (29) J. Liu, J. W. Y. Lam, and B. Z. Tang, "Aggregation-induced emission of silole molecules and polymers: fundamental and applications," *J. Inorg. Organomet. Polym.* **19**(3), 249–285 (2009).
- (30) Z. Zhao, B. He, and B. Z. Tang, "Aggregation-induced emission of siloles," *Chem. Sci.* **6**(10), 5347–5365 (2015).
- (31) J. C. Y. Ng et al., "Valine-containing silole: synthesis, aggregation-induced chirality, luminescence enhancement, chiral-polarized luminescence and self-assembled structures," *J. Mater. Chem. C* **2**(23), 4615–4621 (2014).
- (32) H. Li et al., "Click synthesis, aggregation-induced emission and chirality, circularly polarized luminescence, and helical self-assembly of a leucine-containing silole," *Small* accepted.
- (33) J. C. Y. Ng et al., "Complexation-induced circular dichroism and circularly polarised luminescence of an aggregation-induced emission luminogen," *J. Mater. Chem. C* **2** (1), 78–83 (2014)
- (34) L. Ding et al., "Concentration effects in solid-state CD spectra of chiral atropisomeric compounds," *New J. Chem.* **35**(9), 1781–1786 (2011).
- (35) H. Li et al., "L-Valine methyl ester-containing tetraphenylethene: aggregation-induced emission, aggregation-induced circular dichroism, circularly polarized luminescence, and helical self-assembly," *Mater. Horiz.* **1**(5), 518–521 (2014).

- (36) H. Li et al., "Aggregation-induced chirality, circularly polarized luminescence, and helical self-assembly of a leucine-containing AIE luminogen," *J. Mater. Chem. C* **3**(10), 2399–2404 (2015).
- (37) H. Li et al., "Synthesis, optical properties, and helical self-assembly of a bivaline-containing tetraphenylethene," *Sci. Rep.* **6**, 19277 (2016).
- (38) H. Zhang et al., "Axial chiral aggregation-induced emission luminogens with aggregation-annihilated circular dichroism effect," *J. Mater. Chem. C* **3**(20), 5162–5166 (2015).
- (39) K. Ren et al., "Whole-Teflon microfluidic chips," *Proc. Natl. Acad. Sci. U. S. A.* **108**(20), 8162–8166 (2011).